Supplemental material of: Principle of Maximum Entanglement Entropy and local physics of Strongly Correlated Materials

Nicola Lanatà,[1] Hugo U. R. Strand,[2,3] Yongxin Yao,[4] and Gabriel Kotliar[1]

[1] *Department of Physics and Astronomy, Rutgers University, Piscataway, New Jersey 08856-8019, USA*
[2] *Department of Physics, University of Gothenburg, SE-412 96 Gothenburg, Sweden*
[3] *Department of Physics, University of Fribourg, CH-1700 Fribourg, Switzerland*
[4] *Ames Laboratory-U.S. DOE and Department of Physics and Astronomy, Iowa State University, Ames, Iowa IA 50011, USA*

(Dated: April 15, 2014)

PACS numbers: 71.27.+a, 03.65.Ud, 74.70.Xa, 05.30.Rt

INTRODUCTION

Here we illustrate benchmark calculations of FeTe [1] and of the elemental cerium [2] that further support the principle of maximum entanglement entropy (PMEE) advanced in the main text. Furthermore, we show that both (i) the crossover between the normal-metal and the Janus phase in the iron chalcogenides and (ii) the γ-α isostructural transition of cerium [2] can be understood very neatly in terms of the behavior of the PMEE local thermodynamical parameters.

Let us consider the reduced density matrix $\hat{\rho}_{\mathcal{S}}$ of a crystal $\mathcal{U}$ in its ground state, i.e., at $T = 0$. As in the main text, we define

$$\hat{\mathcal{F}}_{\mathcal{S}} \equiv -\ln \hat{\rho}_{\mathcal{S}} + k \,, \tag{1}$$

where k is a constant defined so that the lowest eigenvalue of $\hat{\mathcal{F}}$ is zero. Within this definition,

$$\hat{\rho}_{\mathcal{S}} \propto e^{-\hat{\mathcal{F}}_{\mathcal{S}}} \,, \tag{2}$$

i.e., $\hat{\mathcal{F}}_{\mathcal{S}}$ represents an effective local Hamiltonian of the $\mathcal{S}$, that is renormalized with respect to the bare local Hamiltonian $\hat{\mathcal{H}}_{\mathcal{S}}$ because of the entanglement with the rest of the system. Interestingly, as we have shown in this work, the effective Hamiltonian $\hat{\mathcal{F}}_{\mathcal{S}}$ depends (approximately) only on few local thermodynamical-like parameters. This finding suggests that, as we are going to argue, these local thermodynamical parameters are the "natural" variables to describe and understand the physics of the $\mathcal{S}$ degrees of freedom.

In order to illustrate the physical meaning of the PMEE local thermodynamical parameters, let us consider the following example. We assume that our crystal $\mathcal{U}$ is in its electronic ground state at a very small volume V, — so that the orbitals that participate to the bonding are very close and the electrons can hop very easily from an atom to the other. Then we transform the system by increasing slowly V (or by increasing the interaction strength U). Since, according to our physical interpretation, the PMEE local thermodynamical parameters defining $\hat{\mathcal{F}}_{\mathcal{S}}$ describe the coupling between $\mathcal{S}$ and the rest of the system, we shall expect that they vary smoothly during this transformation. As we are going to show, this expectation is well founded and physically interesting. In fact, $\hat{\rho}_{\mathcal{S}}$ can have a critical behavior even if the PMEE local thermodynamical parameters vary smoothly during the transformation, merely because of the exponential form of $\hat{\rho}_{\mathcal{S}}$ in relation with the discrete structure of the spectrum of $\hat{\mathcal{F}}_{\mathcal{S}}$, see Eq. (2).

BEHAVIOR OF THE d ELECTRONS IN THE IRON CHALCOGENIDES

In this subsection we describe the physics of the d electrons in the iron chalcogenides making use of the PMEE. For this purpose we focus on FeSe, that was considered also in the main text.

In order to describe the qualitative behavior of $\hat{\rho}_{\mathcal{S}}$ we make use of the Δ_2 PMEE ansatz, which, as shown in Fig. 2 of the main text, is sufficient to capture the local physics of the d electrons within an error $\lesssim 10\%$ in trace-distance, and with even higher precision at $U \simeq 4\,eV$ — that is the physical regime of FeSe.

In the upper panel of Fig. 1 is shown the evolution of the Δ_2 fitting parameters as a function of U, i.e., the coefficients λ_n defining

$$\begin{aligned} \hat{\mathcal{F}}^{(2)}_{\mathcal{S}} \;&\equiv\; \frac{\lambda_{\rm int}}{U}\,\hat{\mathcal{H}}_{\rm int} + \lambda_{x^2-y^2}\,\hat{n}_{x^2-y^2} + \lambda_{z^2}\,\hat{n}_{z^2} \\ &+\; \lambda_{xz,yz}\,\hat{n}_{xz,yz} + \lambda_{xy}\,\hat{n}_{xy}\,, \end{aligned} \tag{3}$$

in the middle panel is shown the corresponding Δ_2 approximation for the entanglement entropy $S^{(2)}$ in comparison with the exact one, and in the lower panel is reported the behavior of the quasi-particle weights (that was shown already in the main text). Note that the factor $1/U$ is present because the interaction operator $\hat{\mathcal{H}}_{\rm int}$ is proportional to U, i.e., the operator $\hat{\mathcal{H}}_{\rm int}/U$ is independent of U.

As anticipated, the Δ_2 fitting parameters λ_n have a very simple behavior: they change monotonically by increasing V, saturate at the crossover point $U \simeq U_c$, and

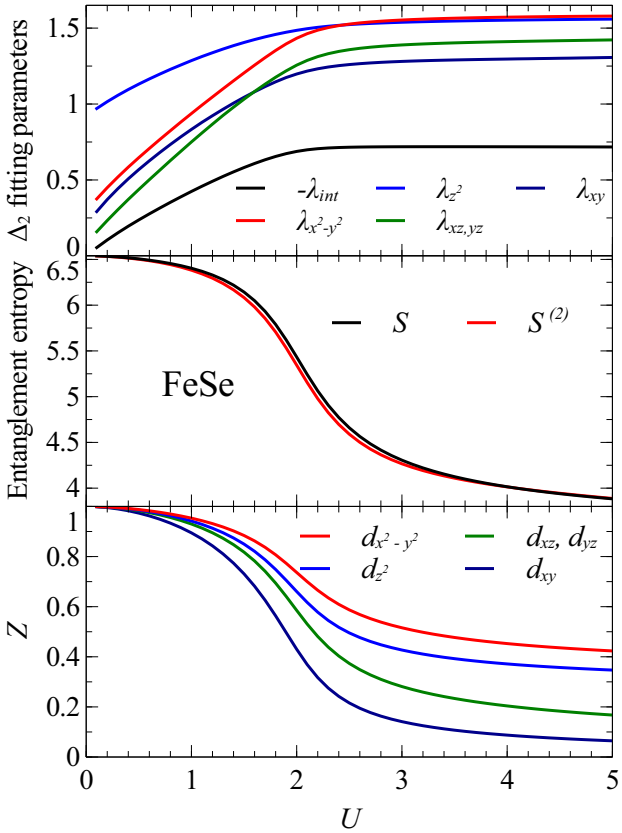

FIG. 1: (Color online) Upper panel: evolution of the Δ_2 PMEE fitting parameters as a function of the volume. Middle panel: evolution of the entanglement entropy for the computed and fitted reduced f density matrices. Lower panel: quasi particle weights.

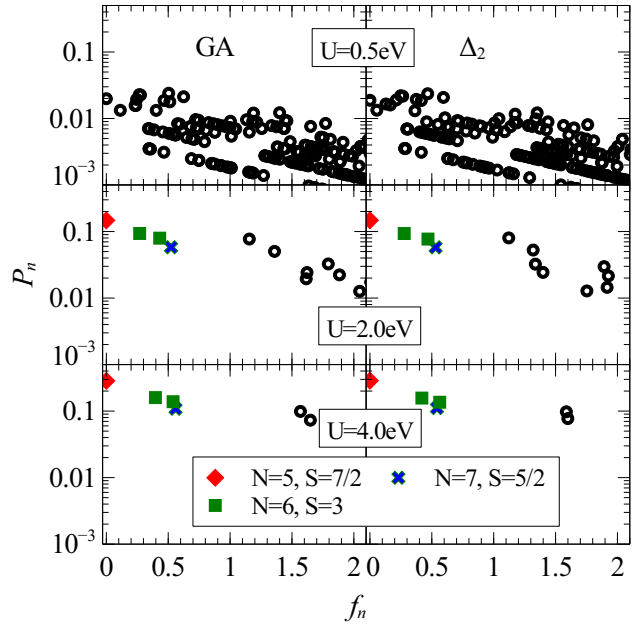

FIG. 2: (Color online) Left panels: GA configuration probabilities $P_n \equiv e^{-f_n}\, d_n$ of the eigenstates of $\hat{\mathcal{F}}_{\mathcal{S}}$ for three values of U (where d_n are the corresponding degeneracies). Right panels: GA configuration probabilities of the eigenstates of $\hat{\mathcal{F}}_{\mathcal{S}}^{(2)}$, see Eq. (3).

remain almost constant at larger U (i.e., in the Janus phase), indicating that $\hat{\rho}_{\mathcal{S}}$ is almost independent of U in this regime. On the contrary, at the crossover point $U \simeq U_c$ between the normal-metal and the Janus phase, — where λ_n vary very slowly — S decreases very rapidly, indicating a rapid change of $\hat{\rho}_{\mathcal{S}}$ characterized by a rapid reduction of the fluctuations of d electrons. Note that the rapid reduction of local d fluctuations is reflected also in the evolution of the quasi-particle weights, that decrease very rapidly at $U \simeq U_c$.

In order to understand more in detail the evolution of $\hat{\rho}_{\mathcal{S}}$, in Fig. 2 are shown the local configuration probabilities of the eigenstates of $\hat{\mathcal{F}}_{\mathcal{S}}$ as a function of their eigenvalues f_n for three values of U, as well as their degeneracies d_n. Interestingly, while at $U \gtrsim U_c$ many multiplets have $f \lesssim 1$, in the Janus phase only the 4 eigenspaces of $\hat{\mathcal{F}}_{\mathcal{S}}$ with the lowest energy are highly populated, and they remain populated within a wide window of U's. Note that, by definition, the configuration probabilities of the eigenstates of $\hat{\mathcal{F}}_{\mathcal{S}}$ decrease exponentially with their eigenvalues f, see Eq. (2). It is for this simple reason that $\hat{\rho}_{\mathcal{S}}$ displays the "critical" behavior discussed above even if the spectrum of $\hat{\mathcal{F}}_{\mathcal{S}}$ varies smoothly as a function of U.

We point out that the reason why the Janus phase is stable within a wide range of U's is that the Hund's coupling reduces the energy-differences between the atomic ground-states with different number of electrons N, i.e., it induces a very small effective Hubbard interaction $U_{\text{eff}} \equiv E_{N=7} + E_{N=5} - 2E_{N=6}$ [3, 4]. This fact has two effects. 1) Since these low-energy local multiplets are close in energy, maintaining finite quantum fluctuations between them have only a small interaction-energy coast even at considerably large U's. 2) Since these multiplets have also different N, as long as the local quantum fluctuations between them are finite the d electrons are free to hop from an atom to another, which increases the bonding energy.

In summary, we have shown that the PMEE local thermodynamical parameters enable to describe very neatly the interplay between the local degrees of freedom of the d electrons and their environment in the iron chalcogenides. In particular, we have shown that the rapid crossover from the normal metallic phase to the Janus phase — which is characterized by a rapid partial localization of the d electrons — is a mere consequence of the generalized Gibbs form of the local reduced density matrix $\hat{\rho}_{\mathcal{S}}$ of the d electrons.

In the next section we are going to show that also the mechanism underlying the iso-structural γ-α volume col-

lapse transition of cerium, see Ref. [2], can be understood very neatly by describing the behavior of the f electrons with the PMEE parameters.

BENCHMARK CALCULATIONS OF THE ELEMENTAL CERIUM: THE γ-α TRANSITION

As a second example, we consider the elemental cerium at zero temperature, which has been recently studied theoretically within the charge self-consistent Local Density Approximation in combination with the GA, see Ref. [2]. In Ref. [2], the important role of the spin-orbit coupling for its γ-α iso-structural transition has been understood by observing the rapid variation of the entanglement entropy of the f electrons, in correspondence of the signature of the γ-α transition — i.e., concomitantly to the minimum of the bulk-modulus $\mathcal{K} = -V dP/dV$.

Let us consider the Δ_2 PMEE approximation $\hat{\rho}_f^{(2)}$ of the f local reduced density matrix $\hat{\rho}_f$. Since in our calculations of cerium the volume is changed keeping the parameters of the on-site interaction constant, it is physically enlightening to represent $\hat{\rho}_f^{(2)}$ as follows,

$$\hat{\rho}_f^{(2)} \propto e^{-\left[\hat{\mathcal{H}}_{\mathcal{S}} + \left(\delta\mu_{5/2}\,\hat{n}_{5/2} + \delta\mu_{7/2}\,\hat{n}_{7/2}\right)\right]/\tau} \,. \tag{4}$$

Equation (4) corresponds to maximize the f entanglement entropy at given average number of 5/2 and 7/2 f-electrons and given expectation-value of $\hat{\mathcal{H}}_{\mathcal{S}} \equiv \hat{\mathcal{H}}^{\rm int} + \hat{\mathcal{H}}^{\rm soc}$; where $\hat{\mathcal{H}}^{\rm int}$ is the Slater interaction with $U = 6\,eV$ and $J = 0.7\,eV$, and $\hat{\mathcal{H}}^{\rm soc}$ is the spin-orbit-coupling (SOC) operator

$$\hat{\mathcal{H}}^{\rm soc} \equiv \mu_{5/2}\,\hat{n}_{5/2} + \mu_{7/2}\,\hat{n}_{7/2} \,, \tag{5}$$

where the coefficients $\mu_{5/2}$ and $\mu_{7/2}$ are obtained from the LDA Kohn-Sham Hamiltonian.

Note that the parameter τ of Eq. (4) is *not* the physical temperature — which is zero by definition in our calculations. In fact, the expectation-value of $\hat{\mathcal{H}}_{\mathcal{S}}$, that is the Legendre-conjugate variable of $\beta_\tau \equiv 1/\tau$, is necessarily always higher than its ground-state energy, as the cerium atoms are not isolated, but they are embedded in the fcc lattice-structure. The parameters $\delta\mu_{5/2}$ and $\delta\mu_{7/2}$ renormalize the bare spin-orbit splitting "experienced" by the f electrons, which is

$$\delta_{\rm soc} \equiv \left(\mu_{7/2} + \delta\mu_{7/2}\right) - \left(\mu_{5/2} + \delta\mu_{5/2}\right) \,. \tag{6}$$

In the upper panel of Fig. 3 is shown the behavior as a function of the volume of Δ_2 and of the fitting parameters τ, $\delta\mu_{5/2}$ and $\delta\mu_{7/2}$. In the lower panel also the evolution of $S[\hat{\rho}_f]$ and $S[\hat{\rho}_f^{(2)}]$ is illustrated. As in Ref. [2], our results are shown both by taking into account the SOC and by neglecting it.

We point out that the PMEE $\hat{\rho}_f^{(2)}$, see Eq. (4), approximates very well the computed reduced density matrix $\hat{\rho}_f$,

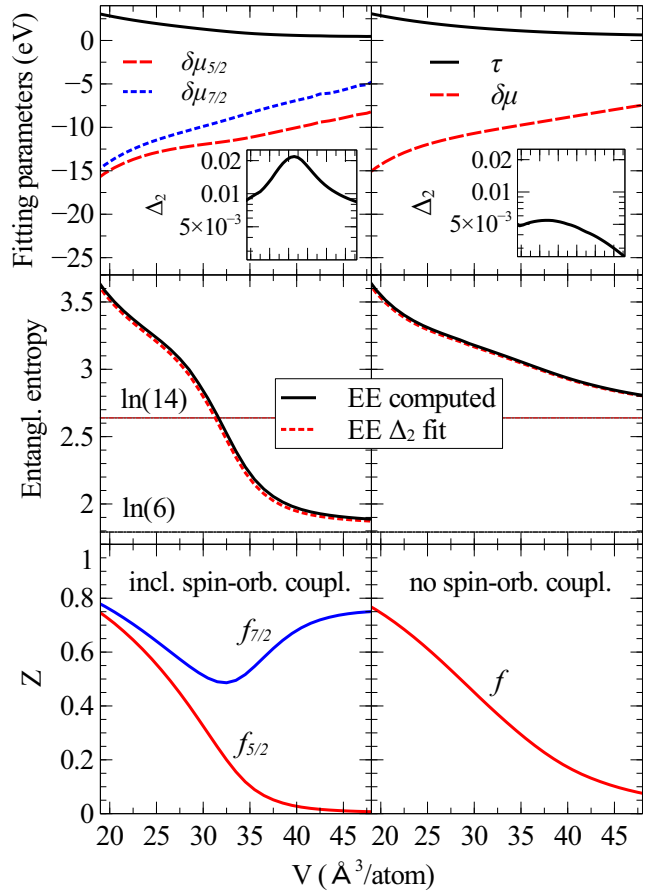

FIG. 3: (Color online) Upper panels: evolution of the Δ_2 PMEE fitting parameters as a function of the volume and corresponding trace-distances (insets). Middle panels: evolution of the entanglement entropy for the computed and fitted reduced f density matrices. Lower panels: quasi particle weights. Our results are shown both with (left panels) and without (right panels) taking into account the spin-orbit coupling.

as indicated by the trace-distance $\Delta_2 \ll 1$. The effective temperature τ decreases by increasing the volume. This is to be expected, as τ reduces to the actual physical temperature $T = 0$ in the infinite-volume limit. On the contrary, at large volumes the renormalized spin-orbit splitting $\delta_{\rm soc}$ becomes considerably larger than $\mu_{7/2} - \mu_{5/2}$, which is of the order of $0.3\,eV$ for all volumes considered (not shown).

Remarkably, although the PMEE fitting parameters vary *smoothly* for all volumes, the entanglement entropy $S[\hat{\rho}_f]$ changes *rapidly* at $V \simeq 33\,\mathring{A}$/atom — i.e., around the minimum of the bulk-modulus $\mathcal{K}$ [2], — indicating that $\hat{\rho}_f$ undergoes a rapid crossover. This observation enables us to ascribe the γ-α transition of cerium to the (approximate) generalized Gibbs form [Eq. (4)] of $\hat{\rho}_f$, and to describe the role of the spin-orbit coupling very neatly as follows. Analogously to a two-level system with a sin-

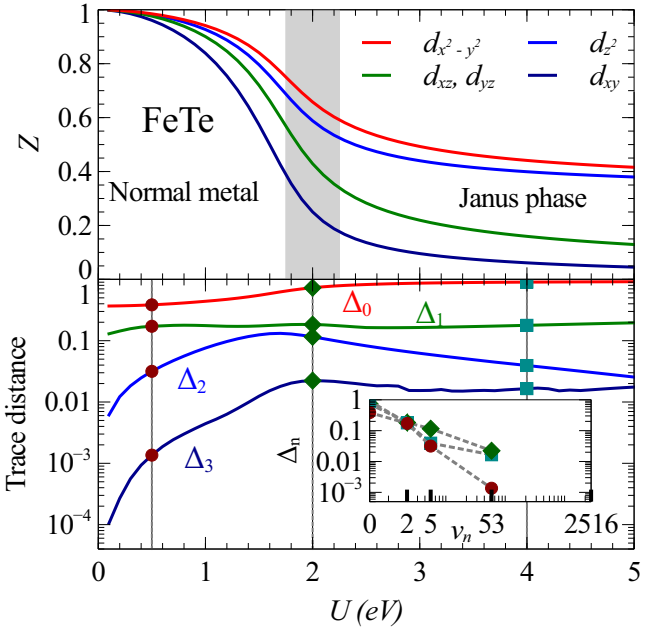

FIG. 4: (Color online) Upper panel: quasi-particle renormalization weights of FeTe. Lower panel: PMEE trace-distances Δ_n for the reduced density matrix ρ_d of FeTe. The insets correspond to $U = 0.5\,eV$, $U = 2\,eV$ and $U = 4\,eV$ at fixed $J/U = 0.224$.

gle particle in thermal equilibrium — in which the equilibrium state undergoes a crossover when the temperature becomes comparable with the energy-gap between the two levels, — the crossover of the reduced density matrix $\hat{\rho}_f$ relates with the *discrete* structure of the spectrum of $\hat{\mathcal{H}}_{\mathcal{S}} + \left(\delta\mu_{5/2}\,\hat{n}_{5/2} + \delta\mu_{7/2}\,\hat{n}_{7/2}\right)$ in relation with the fictitious temperature τ.

The physical picture outlined above might be applicable to describe the volume-collapse transitions in $4f$ and $5f$ systems in general, which is a major subject of investigation in condensed matter physics.

BENCHMARK CALCULATIONS OF FETE

In the upper panel of Fig. 4 the quasi-particle renormalization weights of FeTe — which are computed within the Gutzwiller approximation (GA), see the main text — are shown as a function of the interaction-strength U, keeping the ratio J/U fixed at 0.224. In the lower panel is illustrated the evolution of the PMEE trace-distances $\Delta_0, \Delta_1, \Delta_2, \Delta_3$. The corresponding series Δ_n is shown explicitly in the inset for three values of U as a function of the respective number ν_n of fitting parameters required. In Fig. 5 are shown the computed GA local configuration probabilities for three values of U in comparison with the local configuration probabilities evaluated using the PMEE density matrices corresponding to the trace-distances Δ_2 and Δ_3.

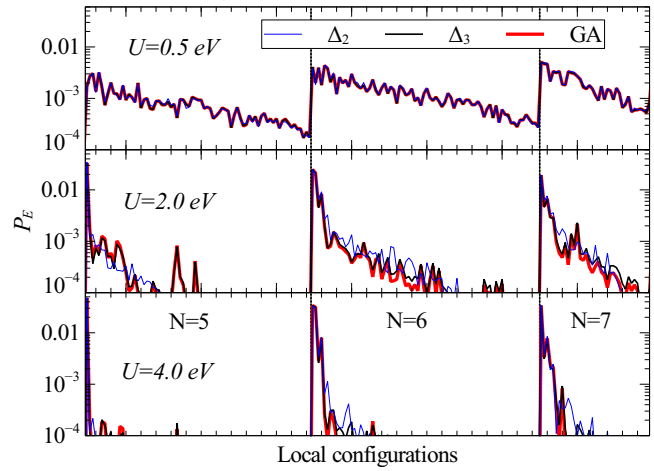

FIG. 5: (Color online) Local configuration probabilities P_E of the eigenstates of $\hat{\mathcal{H}}_{\mathcal{S}}$ of FeTe, in the sectors $N = 5, 6, 7$, for $U = 0.5\,eV$, $U = 2\,eV$ and $U = 4\,eV$. The GA configuration probabilities (red line) are shown in comparison with the local configuration probabilities evaluated using the PMEE density matrices corresponding to the distances Δ_2 and Δ_3. The configuration probabilities P_E are sorted in ascending order of energy. All the calculations are performed at fixed $J/U = 0.224$.

Our results for FeTe are qualitatively identical to those of FeSe discussed in the main text, and further confirm the goodness of our PMEE.

[1] N. Lanatà, H. U. R. Strand, G. Giovannetti, B. Hellsing, L. de' Medici, and M. Capone, Phys. Rev. B **87**, 045122 (2013).

[2] N. Lanatà, Y. X. Yao, C. Z. Wang, K. M. Ho, J. Schmalian, K. Haule, and G. Kotliar, Phys. Rev. Lett. **111**, 196801 (2013).

[3] L. de' Medici, J. Mravlje, and A. Georges, Phys. Rev. Lett. **107**, 256401 (2011).

[4] H. U. R. Strand, ArXiv e-prints (2013), 1303.4215.